Bioorganic Chemistry 87 (2019) 142–154

Contents lists available at ScienceDirect

Bioorganic Chemistry

journal homepage: www.elsevier.com/locate/bioorg

Synthesis of C—C, C—N coupled novel substituted dibutyl benzothiazepinone derivatives and evaluation of their thrombin inhibitory activity

C.P. Baburajeev[a,1], Chakrabhavi Dhananjaya Mohan[b,1], Vijay Pandey[c], Shobith Rangappa[d], Naveen Shivalingegowda[e], Leen Kalash[f], Sannaningaiah Devaraja[g], Andreas Bender[f], Peter E. Lobie[c], Kanchugarakoppal S. Rangappa[h,*], Basappa[a,i,*]

[a] Department of Chemistry, Bangalore University, Central College Campus, Palace Road, Bangalore 560001, India
[b] Department of Studies in Molecular Biology, University of Mysore, Manasagangotri, Mysore 570006, India
[c] Tsinghua Berkeley Shenzhen Institute, Tsinghua University, Shenzhen, Guangdong, PR China
[d] Adichunchanagiri Institute for Molecular Medicine, BG Nagara-571448, Nagamangala Taluk, Mandya District, India
[e] Department of Studies in Physics, University of Mysore, Manasagangotri, Mysore 570006, India
[f] Centre for Molecular Informatics, Department of Chemistry, University of Cambridge, Lensfield Road, Cambridge, United Kingdom
[g] Department of Studies and Research in Biochemistry, Tumkur University, Tumkur 572101, India
[h] Institution of Excellence, Vijnana Bhavan, University of Mysore, Manasagangotri, Mysore 570006, India
[i] Department of Studies in Organic Chemistry, University of Mysore, Manasagangotri, Mysore 570006, India

ARTICLE INFO

Keywords:
Thromboembolic disorder
Antiplatelet
Platelet aggregation
Thrombin inhibitor
Benzothiazepinone

ABSTRACT

The formation of a thrombus is a key event in thromboembolic disorders, that contribute to high mortality and morbidity in affected patients. In the present study, we synthesized a library of novel substituted 3,3-dibutyl-8-methoxy-2,3-dihydrobenzo [b] [1,4] thiazepin-4(5H)-one derivatives which were tested for their platelet aggregation and thrombin inhibitory activity. Among the tested compounds, 3,3-dibutyl-7-(2-chlorophenyl)-8-methoxy-2,3-dihydrobenzo[b] [1,4]thiazepin-4(5H)-one (DCT) displayed the maximum thrombin inhibition with an IC_{50} value of 3.85 μM and thus DCT was chosen for further studies. Next, the effect of DCT on primary hemostasis was evaluated using agonist-induced platelet aggregation model. The lead compound inhibited the collagen- or ADP- or thrombin-induced platelet aggregation in a dose-dependent manner. Furthermore, DCT prolonged the process of clot formation when evaluating plasma re-calcification time (320 ± 11 sec at 5 μg DCT), activated partial thromboplastin time (58.0 ± 0.01 sec at 2 μg), and prothrombin time (14.7 ± 0.01 sec at 5 μg). Molecular docking studies suggested that the benzothiazepinones evaluated here consistently display hydrogen bonding with Ser214 of thrombin, which is similar to that of the co-crystallized ligand (1-(2R)-2-amino-3-phenyl-propanoyl-N-(2,5dichlorophenyl)methylpyrrolidine-2-carboxamide). DCT displayed additional hydrogen bonding to Ser195 and π-π interactions between its methoxyphenyl groups and Trp60, thereby providing a structural rationale for the observed biological effect.

1. Introduction

Thromboembolism is characterized by dislodging of a blood clot (thrombus) from the initial clotting site and circulated to obstruct another blood vessel. Thromboembolic disorders contribute to high mortality and morbidity and they are often associated with excessive stimulation of the coagulation cascade [1]. Thrombin, a serine protease identified as one of the major coagulation factors associated with progression of thromboembolic disorders [2]. Conversion of prothrombin to thrombin followed by thrombin-catalyzed proteolytic cleavage of fibrinogen to insoluble fibrin is the critical event in the activation of coagulation [3]. Thrombin is one of the favorable targets for the development of anticoagulants and rapid translation to clinical practice [4]. Also, thrombin activates several proteins involved in activation of platelets and their aggregation which contributes to upregulated coagulation [5]. The management of coagulation includes the administration of anticoagulants (heparin, low-molecular-weight heparin; warfarin, rivaroxaban), thrombolytic agents (tissue plasminogen activator, streptokinase, urokinase) and surgical interventions [6]. However, the use of heparin, warfarin (4-hydroxy-coumarin derivative),

* Corresponding authors at: Department of Studies in Organic Chemistry, University of Mysore, Manasagangotri, Mysore 570006, India (Basappa).
E-mail addresses: rangappaks@gmail.com (K.S. Rangappa), basappa.uom@gmail.com (Basappa).
[1] These authors contributed equally to this manuscript.

https://doi.org/10.1016/j.bioorg.2019.03.004
Received 29 June 2018; Received in revised form 31 January 2019; Accepted 2 March 2019
Available online 05 March 2019
0045-2068/

streptokinase and urokinase suffers from several disadvantages. Heparin has the requirement of inconvenient parenteral administration and the use of warfarin demands steady vigilance and determination of blood plasma levels [7,8]. Previous findings also suggested that heparin possesses reduced efficacy for the inhibition of fibrin-bound thrombin which may further trigger the growth of a thrombus [9]. The use of streptokinase possesses the risk of immune reactions, while urokinase has limited availability and appears cost-ineffective [10,11]. These drawbacks in a regimen of thromboembolic disorders led to the parallel discovery and development of new direct thrombin inhibitors (DTI) such as hirudin, bivalirudin, dabigatran, argatroban, and melagatran [9]. Unfortunately, dabigatran is associated with an increased risk of myocardial infarction or acute coronary syndrome in a broad spectrum of patients [12]. Ximelagatran is a prodrug of melagatran, which was reported to transiently and asymptomatically elevate levels of the alanine aminotransferase to more than three times the upper limit of normal [13]. The increase in ximelagatran mediated ALT levels may produce hepatotoxicity after long-term intake [14]. Recently, oral thrombin inhibitor treatment was reported to aggravate platelet adhesion and aggregation during arterial thrombosis that might contribute to the increase in acute coronary syndromes observed clinically in patients [15]. The same study also revealed that oral thrombin inhibitor treatment increases thrombus formation and its stability during arterial thrombosis in mice. It was also demonstrated that the prothrombotic action of oral thrombin inhibitor is not due to thrombin-mediated coagulation suggesting the negative side of oral thrombin inhibitors [15]. These findings suggest that it is essential to examine the prothrombotic effect of thrombin inhibitors before their translation into the clinic. Undeniably, anticoagulants with fewer complications are required. Based on the above observations, it is reasonable to postulate that the design of synthetic, orally administrable, bioactive, direct thrombin inhibitor with lesser adverse effects may provide substantial clinical benefit for patients with thromboembolic disorders.

Benzothiazepinone is one of the privileged heterocycles in the medicinal chemistry due to its broad range of pharmacological properties [16–18]. Several research groups have proposed various synthetic routes for the preparation of benzothiazepinone derivatives [19–22]. Previous report reveals that benzothiazepinone derivative TA-993 [(-)-cis-3-acetoxy-5-(2-(dimethylamino)ethyl)-2, 3-dihydro-8-methyl-2-(4-methylphenyl)-1,5-benzothiazepin-4(5H)-one maleate] inhibited platelet aggregation [23] while diltiazem is a benzothiazepine derivative that exhibited antiaggregatory properties in platelets [24–26]. MB3, a metabolite of diltiazem, inhibited aggregation of platelet-induced by collagen, ADP, epinephrine, platelet activating factor, arachidonic acid, and U-46619 in human platelets *in vitro* [27]. Clentiazem (a diltiazem derivative) and its metabolites possess inhibitory activities on platelet aggregation [28]. Moreover, diltiazem is well-documented as a calcium channel blocker in myocardial and vascular smooth muscle cells and used in the treatment of hypertension, and angina pectoris [29,30]. The structures of TA-993, diltiazem and MB3 are presented as Fig. 1. The underlying molecular mechanism of antiaggregatory property of benzothiazepinone in platelets remained unclear. It is essential note that, the aforementioned compounds were structurally altered on the 7-membered ring while the aromatic ring remained untouched. In addition, most of the previously studied benzothiazepinone (TA-993, diltiazem, MB3) possess unstable α-hydroxyl amides in the 7-membered ring. Therefore, in the present report, we synthesized a library of novel 3,3-dibutyl-8-methoxy-2,3-dihydrobenzo [b] [1,4] thiazepin-4(5H)-one derivatives by introducing various substituents on the aromatic ring and dibutyl group at the α-position of the amide chain that makes the structure relatively more stable. The new compounds are screened for their platelet aggregation and thrombin inhibitory activity.

2. Material and methods

All organic chemicals used were purchased from Sigma-Aldrich. ^{1}H and ^{13}C NMR spectra were recorded on a Bruker WH-200 (400 MHz) and JEOLJSM-ECS (400 MHz), spectrometer in $CDCl_3$ or DMSO-d_6 as a solvent, using TMS as an internal standard and chemical shifts are expressed as ppm. High-resolution mass spectra were determined on a WATERS Q-TOF Premier-HAB213 instrument. Mass spectra were determined on an Agilent LC-MS and the elemental analyses were carried out using an Elemental Vario Cube CHNS rapid Analyzer. Collagen type-I, ADP, and thrombin were purchased from Sigma Chemicals Company, St. Louis, USA. Uniplastin, Liquicelin-E, and Fibroquant were purchased from Tulip Diagnostics Pvt. Ltd., Goa, India. All other chemicals and reagents used were analytical grade. Thrombin Inhibitor Screening Kit (Catalog #: K374) was purchased from BioVision, Inc. A fresh blood sample was collected from healthy human donors. All the experimental protocols were approved by the Institutional Human Ethical Committee, University of Mysore, Mysuru and the experiments are conducted in accordance with the ethical guidelines.

2.1. Chemistry

2.1.1. Typical procedure for the synthesis of 3,3-dibutyl-8-methoxy-2,3-dihydrobenzo[b] [1,4]thiazepin-4(5H)-one (1)

2-(bromomethyl)-2-butylhexanoic acid (2.65 g; 0.01 mol) and potassium-2-amino-5-methoxy benzenethiolate (2.88 g; 0.015 mol) was dissolved in 30 ml of THF at room temperature. The reaction mass was heated at 60 °C for 3 h and the completion of the reaction was monitored by TLC. The reaction mass was quenched in water, the pH is adjusted to between 6 and 7 and extracted with ethyl acetate. The combined organic phase was washed with brine to remove THF, dried over anhydrous sodium sulfate and concentrated under vacuum to obtain a brown liquid product with 85% yield. Thereafter, liquid product along with DMF (30 ml), TEA (1.01 g; 0.01 mol), benzotriazol -1-yloxytris(dimethylamino)phosphonium hexafluorophosphate (BOP)

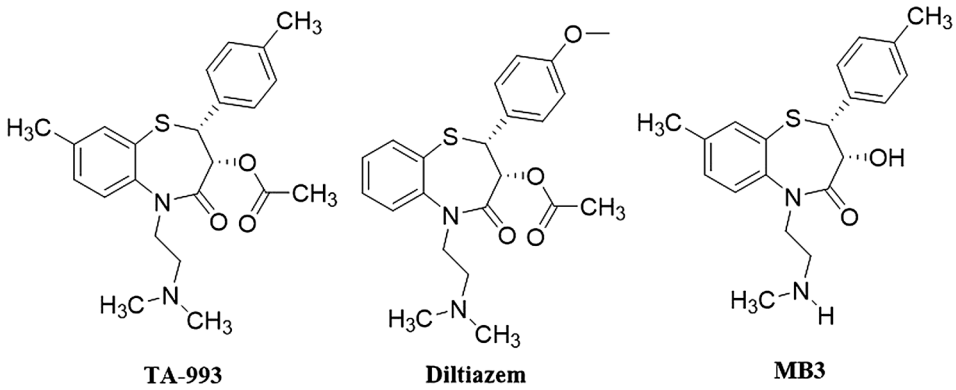

Fig. 1. Structure of known benzothiazepinone derivatives that possess antiaggregatory properties in platelets.

(2.21 g; 0.5 mol) and $NaHCO_3$ (10%) was stirred for 3 h. After the reaction time, reaction mass diluted and extracted with ethyl acetate (50 ml). The organic layer was washed with brine, dried over anhydrous sodium sulfate and the solvent was removed in vacuum to obtain 3,3-dibutyl-8-methoxy-2,3-dihydrobenzo[b] [1,4]thiazepin-4(5H)-one (**1**) as brown solid (2.56 g) with a yield of 80%.

*2.1.2. Typical procedure for the synthesis of 3,3-dibutyl-7-iodo-8-methoxy-2,3-dihydrobenzo[b] [1,4]thiazepin-4(5H)-one (**2**)*

To a solution of compound **1** (3.21 g; 0.01 mol) in CH_3CN/H_2O (1:30 ml), 1,4-bis(triphenylphosphonium)-2-butene peroxodisulfate (5.8 g; 0.01 mol) and iodine (1.27 g; 0.01 mol) was added and the reaction mixture was stirred at ambient temperature for 3 h. The progress of the reaction was monitored using TLC. The reaction mixture was poured into an aqueous sodium thiosulfate solution (3.2 g in 20 ml water) and extracted with ethyl acetate. The organic layer was concentrated and the obtained crude product was purified using column chromatography using *n*-hexane/ethyl acetate as eluent to get iodinated product (**2**) with a yield (3.5 g) of 71%.

*2.1.3. 3,3-dibutyl-7-iodo-8-methoxy-2,3-dihydrobenzo[b] [1,4]thiazepin-4(5H)-one (**2**)*

Off-white solid; mp 146–147 °C; ^{1}H NMR (400 MHz, DMSO-d_6) δ: 9.57 (s, 1H), 7.32 (s, 1H), 7.09 (s, 1H), 3.81 (s, 3H), 2.98 (s, 2H), 1.66–1.59 (m, 2H), 1.50–1.43 (m, 2H), 1.20–1.16 (m, 8H), 0.83–0.80 (t, 6H); ^{13}C NMR (100 MHz, DMSO-d_6) δ: 175.8, 150.8, 134.9, 128.6, 125.4, 115.2, 109.9, 87.6, 56.5, 51.7, 41.5, 37.6, 25.5, 22.6, 13.7; HRMS Calcd 470.0621; Found: 470.0622 (M + Na^+).

2.1.4. General procedure for C−N bond-formation reaction

The reaction flask was charged with substrate **2** (447 mg; 1 mmol), amines (**3a-i**) (1 mmol), 1,3-Bis(2,4,6-trimethylphenyl)imidazolinium Chloride (L4) (35 mg, 0.1 eq), $Pd_2(dba)_3$ (45 mg; 0.05 eq), and Cs_2CO_3 (143 mg; 2.5 eq) followed by the addition of reagent grade 1,4 dioxane (5 ml). The reaction mixture was heated at 100 °C for 12 h. After the completion of reaction, the mixture was cooled to room temperature, quenched with water and diluted with ethyl acetate (10 ml) and the aqueous layer was extracted with ethyl acetate (30 ml). The combined organic layer was washed with water, dried over anhydrous sodium sulfate and the solvent was removed in vacuum. The crude product was purified using silica gel column chromatography using *n*-hexane/ethyl acetate as eluent to get final product (**4a-i**).

*2.1.4.1. 3,3-dibutyl-8-methoxy-7-(phenylamino)-2,3-dihydrobenzo[b] [1,4]thiazepin-4(5H)-one (**4a**)*. Yield 80% (329.6 mg); Off-white colored solid; mp 135–146 °C; ^{1}H NMR (400 MHz, $CDCl_3$); 7.49–7.27 (m, 6H), 7.04 (s, 1H), 6.90 (s, 1H), 3.80 (s, 3H), 3.02 (s, 2H), 1.85–1.81 (m, 2H), 1.65–1.61 (m,2H), 1.31–1.25 (m, 8H), 0.97–0.87 (m, 6H); ^{13}C NMR (100 MHz, $CDCl_3$); 177.2, 152.5, 136.9, 133.0, 129.2, 128.1, 127.4, 123.7, 114.6, 56.0, 52.3, 41.5, 38.3, 29.6, 26.0, 23.2, 13.9; LCMS (MM: ES + APCI) 413.4 (M + H)$^+$.

*2.1.4.2. 3,3-dibutyl-8-methoxy-7-(p-tolylamino)-2,3-dihydrobenzo[b] [1,4]thiazepin-4(5H)-one (**4b**)*. Yield 79% (340.8 mg); White colored solid; mp 146–147 °C; ^{1}H NMR (400 MHz, DMSO-d_6); 9.34 (s, 1H), 7.36 (s,1H), 7.04–7.03 (m, 4H), 6.96–6.95 (d, J = 4 Hz, 1H), 6.89–6.88 (d, J = 4 Hz, 1H), 3.81 (s, 3H), 2.96 (s, 2H), 2.24 (s, 3H), 1.83–1.43 (m, 4H), 1.17 (m, 8H), 0.82 (m, 6H); ^{13}C NMR (100 MHz, DMSO-d_6); 175.8, 144.2, 135.0, 129.6, 129.3, 118.8, 116.2, 114.2, 107.3, 55.7, 51.6, 44.1, 25.7, 22.8, 20.2, 13.8; LCMS (MM: ES + APCI) 427.4 (M + H)$^+$.

*2.1.4.3. 3,3-dibutyl-8-methoxy-7-((4-methoxyphenyl)amino)-2,3-dihydrobenzo[b] [1,4]thiazepin-4(5H)-one (**4c**)*. Yield 80% (353.7 mg); White colored solid; mp 166–167 °C; ^{1}H NMR (400 MHz, DMSO-d_6); 9.60 (s, 1H), 7.44–7.42 (d, J = 8.0 Hz, 2H), 7.35–7.31 (m, 3H), 7.22 (s, 1H), 6.82 (s, 1H), 3.85 (s, 3H), 3.83 (s,3H), 2.99 (s, 2H), 1.67–1.59 (m, 2H), 1.51–1.44 (m, 2H), 1.30–1.21 (m, 8H), 0.85 (m, 6H); HRMS Calcd 465.2182; Found: 465.2185 (M + Na^+); Anal.Calcd for $C_{25}H_{34}N_2O_3S$: C, 67.84; H 7.74; N 6.33; Found: C, 67.89; H, 7.69; N, 6.36.

*2.1.4.4. 3,3-dibutyl-7-((4-chlorophenyl)amino)-8-methoxy-2,3-dihydrobenzo[b] [1,4]thiazepin-4(5H)-one (**4d**)*. Yield 78% (348.6 mg); White colored solid; mp 172–173 °C; ^{1}H NMR (400 MHz, DMSO-d_6); 9.43 (s, 1H), 7.74 (s,1H), 7.25–7.23 (d, J = 8.0 Hz, 2H), 7.11–7.09 (d, J = 8.0 Hz, 2H), 7.01 (s, 1H), 6.97 (s, 1H), 3.82 (s, 3H), 2.98 (s, 2H), 1.58–1.47 (m, 4H), 1.18–1.16 (m, 8H), 0.85–0.82 (m, 6H); ^{13}C NMR (100 MHz, DMSO-d_6); 174.2, 153.7, 137.1, 136.5, 131.9, 131.7, 130.1, 128.5, 116.6, 110.3, 56.5, 50.6, 45.7, 22.7, 13.7; LCMS (MM: ES + APCI) 447.2 (M + H)$^+$.

*2.1.4.5. 3,3-dibutyl-8-methoxy-7-((2-methoxyphenyl)amino)-2,3-dihydrobenzo[b] [1,4]thiazepin-4(5H)-one (**4e**)*. Yield 76% (336 mg); Off-white colored solid; mp 151–152 °C; ^{1}H NMR (400 MHz, DMSO-d_6); 9.51 (s, 1H), 7.30–7.26 (m, 2H), 7.05–7.04 (d, J = 8 Hz, 1H), 6.96–6.86 (m, 4H), 3.73 (s, 3H), 3.71 (s, 3H), 2.98 (s, 2H), 1.59 (m, 2H), 1.48 (m, 2H), 1.18–1.14 (m, 8H), 0.80 (m, 6H); ^{13}C NMR (100 MHz, DMSO-d_6); 176.4, 159.4, 152.1, 138.8, 134.7, 130.1, 129.6, 128.6, 124.1, 121.8, 115.3, 115.1, 56.4, 55.5, 52.08, 42.2, 38.2, 26.1, 23.3, 14.4. LCMS (MM: ES + APCI) 443.4 (M + H)$^+$.

*2.1.4.6. 3,3-dibutyl-7-((2-chlorophenyl)amino)-8-methoxy-2,3-dihydrobenzo[b] [1,4]thiazepin-4(5H)-one (**4f**)*. Yield 75% (334 mg); White colored solid; mp 167–168 °C; ^{1}H NMR (400 MHz, $CDCl_3$); 7.47–7.43 (d, J = 8 Hz, 1H), 7.43–7.42 (d, J = 8.0 Hz, 1H), 7.29–7.22 (m, 4H), 7.02 (s, 1H), 6.77 (s, 1H), 3.75 (s, 3H), 3.02 (s, 2H), 1.84–1.77 (m, 2H), 1.64–1.58 (m, 2H), 1.25–1.24 (m, 8H), 0.88–0.84 (m, 6H); ^{13}C NMR (100 MHz, $CDCl_3$); 177.3, 153.0, 136.1, 133.8, 132.9, 131.5, 130.0, 129.5, 129.0, 128.9, 126.6, 124.1, 114.6, 56.1, 52.2, 41.8, 38.3, 26.1, 23.3, 14.0; LCMS (MM: ES + APCI) 448.4 (M + H)$^+$.

*2.1.4.7. 3,3-dibutyl-8-methoxy-7-((4-methylpyridin-2-yl)amino)-2,3-dihydrobenzo [b] [1,4] thiazepin-4(5H)-one (**4g**)*. Yield 61% (260.8 mg); Off-White colored solid; mp 136–137 °C: ^{1}H NMR (400 MHz, DMSO-d_6); 9.34 (s, 1H), 8.05 (d, 1H), 7.54 (m, 3H), 7.36 (s, 1H), 7.29 (s, 1H), 3.81 (s, 3H), 2.96 (s, 2H), 2.24 (s, 3H), 1.54–1.45 (m, 4H), 1.20–1.11 (m, 8H), 0.85 (m, 6H); LCMS (MM: ES + APCI) 428.4 (M + H)$^+$. Anal.Calcd for $C_{24}H_{33}N_3O_2S$: C 67.41, H 7.78, N 9.83; Found: C, 67.48; H, 7.71; N, 9.89.

2.1.4.8. 2-(2-chloro-4-((3,3-dibutyl-8-methoxy-4-oxo-2,3,4,5-tetrahydrobenzo [b] [1,4]thiazepin-7-yl)amino)-5-methylphenyl)-2-(4-chlorophenyl)acetonitrile (4h). Yield 63% (383.7 mg); Off-White colored solid; mp 141–142 °C; ^{1}H NMR (400 MHz, DMSO-d_6); 9.38 (s, 1H), 7.49–7.47 (d, J = 8.0 Hz, 2H), 7.40–7.33 (m, 5H), 7.28 (s, 1H), 7.05 (s, 1H), 6.31 (s, 1H), 3.88 (s, 3H), 3.01 (s, 2H), 2.30 (s, 3H), 1.60–1.48 (m, 4H), 1.21–1.13 (m, 8H), 0.87–0.83 (m, 6H); ^{13}C NMR (100 MHz, DMSO-d_6); 175.8, 144.3, 142.3, 135.2, 134.8, 126.9, 126.6, 116.8, 114.4, 108.1, 55.8, 41.6, 44.0, 40.1, 37.2, 25.7, 22.7, 13.8, 13.4; LCMS (MM: ES + APCI) 610.2 (M + H)$^+$.

*2.1.4.9. 3′-((3,3-dibutyl-8-methoxy-4-oxo-2,3,4,5-tetrahydrobenzo[b] [1,4]thiazepin-7-yl)amino)-[1,1′-biphenyl]-2-carbonitrile (**4i**)*. Yield 65% (333.5 mg); Off-white colored solid; mp 143–144 °C; ^{1}H NMR (400 MHz, DMSO-d_6); 9.51 (s, 1H), 7.43–7.40 (m, 6H), 7.34–7.32 (m, 3H), 7.21 (s, 1H), 6.81 (s, 1H), 3.83 (s, 3H), 3.02 (s, 2H), 1.63–1.59 (m, 4H), 1.12–1.11 (m, 8H), 0.82–0.78 (m, 6H); LCMS (MM:ES + APCI) 514.4 (M + H)$^+$. Anal.Calcd for $C_{31}H_{35}N_3O_2S$: C, 72.48; H, 6.87; N, 8.18; Found: C, 72.51; H, 6.83; N, 8.14.

2.1.5. General procedure for C−C bond-formation reaction

The reaction flask was charged with substrate **2** (447 mg; 1 mmol), boronic acid **(5a-i)** (1 mmol), 2,2′-bis(diphenylphosphino)-1,1′-

binaphthyl (L3) (62.2 mg; 0.1 eq), $Pd(PPh)_3Cl_2$ (35.1 mg; 0.05 eq), and Cs_2CO_3 (142 mg; 2.5 eq) followed by the addition of reagent grade 1,4 dioxane (5 ml). The reaction mixture was heated at 100 °C for 8 h. After the completion of reaction, mixture is cooled to room temperature, quenched with water and diluted with ethyl acetate (10 ml) and the aqueous layer was extracted with ethyl acetate (30 ml). The combined organic layer was washed with water, dried over anhydrous sodium sulfate and the solvent was removed in vacuum. The crude product was purified using silica gel column chromatography using *n*-hexane/ethyl acetate as eluent to get final product (**6a-i**). All the new compounds exhibited spectral properties consistent with the assigned structures and were fully characterized by their spectroscopic methods (^{1}H, IR, Mass, elemental and ^{13}C NMR analysis).

*2.1.5.1. 3,3-dibutyl-8-methoxy-7-phenyl-2,3-dihydrobenzo[b] [1,4] thiazepin-4(5H)-one (**6a**)*. Yield 84% (333.6 mg); White colored solid; mp 154–155 °C; ^{1}H NMR (400 MHz, DMSO-d_6); 9.52 (s, 1H), 7.38–7.28 (m, 5H), 7.06–7.02 (2H), 3.79 (s, 3H), 2.99 (s, 2H), 1.61–1.59 (m, 2H), 1.49–1.47 (m, 2H), 1.19–1.15 (m, 8H), 0.80–0.78 (m, 6H); ^{13}C NMR (100 MHz, $CDCl_3$); 176.4, 152.1, 137.5, 134.7, 130.4, 129.5, 128.6, 127.7, 124.1, 115.1, 56.4, 52.1, 42.2, 38.2, 26.1, 23.3, 14.4. LCMS (MM: ES + APCI) 398.4 $(M + H)^+$.

*2.1.5.2. 3,3-dibutyl-7-(4-chloro-3-(trifluoromethyl)phenyl)-8-methoxy-2,3-dihydrobenzo [b] [1,4] thiazepine-4(5H)-one (**6b**)*. Yield 81% (404.3 mg); White colored solid; mp 184–186 °C; ^{1}H NMR (400 MHz, $CDCl_3$); 8.05 (s, 1H), 7.80–7.79 (d, J = 4 Hz, 1H), 7.60–7.57 (dd, J_1 = 4 Hz, J_2 = 4 Hz, 2H), 7.02 (s, 1H), 7.93 (s, 1H), 3.79 (s, 3H), 2.93 (s, 2H), 1.87–1.79 (m, 2H), 1.64–1.57 (m, 2H), 1.23–1.22 (m, 8H), 0.86–0.82 (m, 6H); ^{13}C NMR (100 MHz, $CDCl_3$); 177.6, 152.2, 136.0, 133.5, 131.2, 130.5, 128.4, 128.1, 123.4, 114.7, 56.1, 52.4, 41.2, 38.5, 26.1, 23.2, 14.0; LCMS (MM: ES + APCI) 500.2 $(M + H)^+$.

*2.1.5.3. 3,3-dibutyl-8-methoxy-7-(3-methoxyphenyl)-2,3-dihydrobenzo[b] [1,4]thiazepin-4(5H)-one (**6c**)*. Yield 83% (354.5 mg); Off-white colored solid; mp 136–138 °C; ^{1}H NMR (400 MHz, DMSO-d_6); 9.55 (s, 1H), 7.32 (m, 1H), 7.10–7.09 (d, J = 4 Hz, 2H), 7.00–6.93 (m, 3H), 3.77 (s, 3H), 3.75 (s, 3H), 3.34 (s, 2H), 1.63 (m, 2H), 1.53 (m, 2H), 1.20 (m, 8H), 0.85–0.82 (m, 6H); ^{13}C NMR (100 MHz, DMSO-d_6); 175.9, 158.8, 151.5, 138.3, 134.1, 129.6, 129.1, 128.1, 123.5, 121.3, 114.7, 112.5, 55.8, 54.9, 51.5, 41.7, 37.6, 25.5, 22.7, 13.8; LCMS (MM: ES + APCI) 428.4 $(M + H)^+$.

*2.1.5.4. 3,3-dibutyl-8-methoxy-7-(4-(trifluoromethyl)phenyl)-2,3-dihydrobenzo[b] [1,4] thiazepin-4(5H)-one (**6d**)*. Yield 81% (376.8 mg); White colored solid; mp 198–199 °C; ^{1}H NMR (400 MHz, $CDCl_3$); 7.93 (s, 1H), 7.65–7.63 (d, J = 8 Hz, 2H), 7.59–7.57 (d, J = 8 Hz, 2H), 7.03 (s, 1H), 6.94 (s,1H), 3.79 (s, 3H), 3.0 (s, 2H), 1.87–1.82 (m, 2H), 1.65–1.59 (m, 2H), 1.31–1.23 (m, 8H), 0.86–0.83 (m, 6H); ^{13}C NMR (100 MHz, $CDCl_3$); 177.6, 152.4, 140.7, 133.4, 130.2, 129.7, 129.3, 125.1, 123.7, 114.7, 56.1, 52.4, 41.3, 38.4, 26.1, 23.2, 14.0; HRMS Calcd 488.1842; Found: 488.1844 $(M + Na^+)$.

*2.1.5.5. 3,3-dibutyl-7-(2-fluorophenyl)-8-methoxy-2,3-dihydrobenzo[b] [1,4]thiazepin-4(5H)-one (**6e**)*. Yield 79% (328 mg); White colored solid; mp 154–156 °C; ^{1}H NMR (400 MHz, DMSO-d_6); 9.63 (s, 1H), 7.48–7.44 (m, 1H), 7.32–7.28 (m, 3H), 7.18 (s,1H), 7.04 (s, 1H), 3.78 (s, 3H), 3.11 (s, 2H), 1.70–1.67(m, 2H), 1.60–1.55 (m, 2H), 1.25 (m, 8H), 0.89–0.87 (m, 6H); ^{13}C NMR (100 MHz, DMSO-d_6); 176.4, 152.5, 134.5, 132.0, 130.2, 130.1, 129.3, 124.9, 124.7, 124.5, 116.0, 115.8, 114.7, 56.4, 52.0, 42.2, 38.0, 26.0, 23.2, 14.3; LCMS (MM: ES + APCI) 416.4 $(M + H)^+$.

*2.1.5.6. 3,3-dibutyl-7-(2-chlorophenyl)-8-methoxy-2,3-dihydrobenzo[b] [1,4]thiazepin-4(5H)-one (**6f**, DCT)*. Yield 80% (344.9 mg); White colored solid; mp 146–147 °C; ^{1}H NMR (400 MHz, DMSO-d_6); 9.55 (s, 1H), 7.32–7.30 (m, 1H), 7.09–7.00 (m, 2H), 6.99–6.96 (s, 2H), 6.90 (s, 1H), 3.75 (s, 3H), 3.0 (s, 2H), 1.67–1.62(m, 2H), 1.55–1.51 (m, 2H), 1.23–1.18 (m, 8H), 0.85 (m, 6H); HRMS Calcd 454.1578; Found: 454.1582 $(M + Na^+)$;. Anal.Calcd for $C_{24}H_{30}ClNO_2S$: C, 66.72; H, 7.00; N, 3.24; Found: C, 66.68; H, 6.97; N, 3.27.

*2.1.5.7. 3,3-dibutyl-8-methoxy-7-(p-tolyl)-2,3-dihydrobenzo[b] [1,4] thiazepin-4(5H)-one (**6g**)*. Yield 83% (341.2 mg); White colored solid; mp 143–144 °C; ^{1}H NMR (400 MHz, $CDCl_3$); 7.63 (s, 1H), 7.47–7.45 (d, J = 8.0 Hz, 1H), 7.41–7.37 (m, 2H), 7.34–7.30 (m,1H), 7.01 (s,1H), 6.90 (s, 1H), 3.78 (s,3H), 3.00 (s, 2H), 2.34 (s, 3H), 1.87–1.79 (m, 2H), 1.65–1.59 (m. 2H), 1.32–1.24 (m, 8H), 0.88–0.84 (m, 6H); ^{13}C NMR (100 MHz, $CDCl_3$); 177.4,152.6, 137.0, 133.2, 131.1, 129.3, 129.2, 128.2, 127.5, 123.8, 114.7, 56.1, 52.4, 41.6, 38.4, 29.7, 26.1, 23.3, 14.0; LCMS (MM: ES + APCI) 412.4 $(M + H)^+$.

*2.1.5.8. 3,3-dibutyl-8-methoxy-7-(4-nitrophenyl)-2,3-dihydrobenzo[b] [1,4]thiazepin-4(5H)-one (**6h**)*. Yield 41% (181.2 mg); Off-white colored solid; mp 139–140 °C; ^{1}H NMR (400 MHz, $CDCl_3$); 8.33–8.31 (d, J = 8.0 Hz, 2H), 7.53–7.47 (m, 3H), 7.03 (s, 1H), 6.84 (s, 1H), 3.77 (s, 3H), 3.01 (s, 2H), 1.86–1.78 (m, 2H), 1.65–1.57 (m, 2H), 1.30–1.24 (m, 8H), 0.88–0.85 (m, 6H); ^{13}C NMR (100 MHz, $CDCl_3$); 177.3, 153.1, 145.9, 132.9, 131.6, 130.1, 129.6, 125.4, 124.3, 123.9, 115.9, 114.6, 56.2, 52.3, 41.6, 38.3, 26.1, 23.2, 14; LCMS (MM: ES + APCI) 443.4 $(M + H)^+$.

*2.1.5.9. 4-(3,3-dibutyl-8-methoxy-4-oxo-2,3,4,5-tetrahydrobenzo[b] [1,4] thiazepin-7-yl) benzonitrile (**6i**)*. Yield 43% (181.5 mg); Off-white colored solid; mp 130–131 °C; ^{1}H NMR (400 MHz, DMSO-d_6); 9.31 (s, 1H), 7.73–7.71 (d, J = 8.0 Hz, 1H), 7.65–7.58 (m, 3H), 7.50 (s, 1H), 7.01 (s, 1H), 3.83 (s, 3H), 3.0 (s, 2H), 1.54–1.39 (m, 4H), 1.23–1.18 (m, 8H), 0.88 (m, 6H); HRMS Calcd 445.1920; Found: 445.1924 $(M + Na^+)$; Anal.Calcd for $C_{25}H_{30}N_2O_2S$: C, 71.06; H, 7.16; N, 6.63; Found: C, 71.10; H, 7.10; N, 6.69.

2.2. Biology

2.2.1. Thrombin inhibition assay

The effect of the newly synthesized compounds on thrombin activity was measured using Thrombin Inhibitor Screening Kit, BioVision, the USA as per the manufacturer's instructions. Briefly, thrombin enzyme solution is prepared with assay buffer and 50 µl of enzyme solution is taken in each well in a 96-well plate. Thereafter enzyme is incubated with new compounds and substrate for 15 min followed by measuring of the fluorescence activity. PPACK dihydrochloride was used as positive control.

2.2.2. Determination of plasma re-calcification time

The plasma re-calcification time was determined as described earlier [31]. Briefly, the DCT (0–5 µg) was pre-incubated with 0.2 ml of citrated human plasma in the presence of 10 mM Tris HCl (20 µl) buffer pH 7.4 for 1 min at 37 °C. Then 0.25 M $CaCl_2$ (20 µl) was added to the pre-incubated mixture and clotting time was recorded.

2.2.3. Determination of activated partial thromboplastin time (APTT) and prothrombin time (PT)

Briefly, 100 µl of normal citrated human plasma and DCT (0–5 µg) were pre-incubated for 1 min at room temperature. Using the coagulation analyzer (Labitec, Germany), APTT and PT performed according to the manufacturer instructions. For APTT, we add 100 µl of Liquicelin-E phospholipids preparation derived from Rabbit brain with ellagic acid. The clotting reaction initiated by adding 100 µl of 0.02 M $CaCl_2$ and the clotting time was measured. For PT, the clotting reaction was initiated by adding 200 µl of PT reagent (Uniplastin–rabbit brain thromboplastin). The period for the visible clot documented in seconds unit. The APTT ratio and the international normalized ratio for PT at

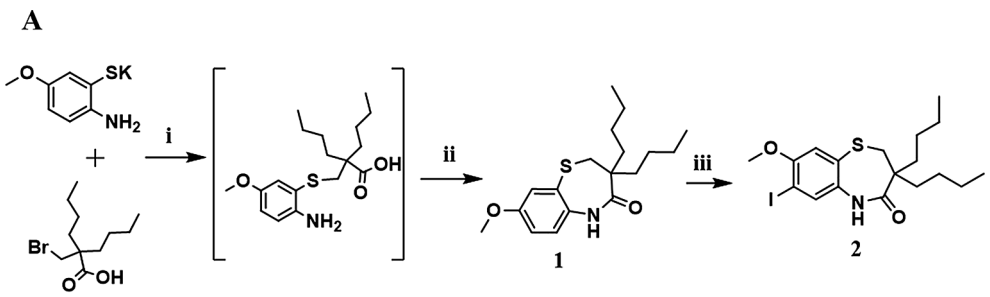

Fig. 2. (A) Scheme for the synthesis of 3,3-dibutyl-7-iodo-8-methoxy-2,3-dihydrobenzo [b] [1,4]thiazepin-4(5H)-one. (B) Structure of the ligands [1,10 -Phenanthroline (L1, Diamine), 2′-(Dicyclohexylphosphino)acetophenone ethylene ketal (L2, BINAP), 2,2′-bis(diphenylphosphino)-1,1′-binaphthyl (L3, Sympos) and 1,3-Bis(2,4,6-trimethylphenyl) imidazolinium Chloride (L4, *N*-heterocyclic carbine)] that were used for the C—N and C—C bond formation reactions.

each point analyzed and from the values of control plasma incubated with the buffer for an equal period.

2.2.4. Determination of thrombin clotting time (TCT)

Thrombin clotting time was determined according to the slightly modified method of Evans. Briefly, 100 µl of human citrated plasma were pre-incubated with DCT (0–5 µg) in 10 mM Tris–HCl buffer pH 7.4 at 37 °C. The clotting time was then determined after adding 100 µl of diluted thrombin (0.5 units/ml) to the 100 µl of incubation sample.

2.2.5. Preparation of platelet-rich plasma and platelet-poor plasma

We employed Ardlie and Han methodology [32] for the preparation of human platelet-rich plasma (PRP) and platelet-poor plasma (PPP). The platelet concentration of PRP adjusted to 3.1×10^8 platelets/ml with PPP. For aggregation process, the PRP maintained at 37 °C was used within two hours. All the above preparations were performed using plastic-wares or siliconized glassware.

2.2.6. Preparation of washed platelets

The method of Born was employed for the preparation of the washed platelets [33]. Acid citrate dextrose buffer 1.5 ml, (containing 2.5 g trisodium citrate dehydrate, 1.4 g of citric acid and 2 g of anhydrous D-glucose, pH 4.5) taken in a plastic centrifuge tube, 9 ml of blood was added and centrifuged for 15 min at 30 g. The supernatant, PRP was transferred into a plastic tube and kept in an incubator at 37 °C for 15 min and then centrifuged for 20 min at 4500g. The pellet collected, and it further suspended in tyrode albumin buffer pH 6.5 (NaCl; 0.16 g, KCl; 0.004 g, $NaHCO_3$; 0.02 g, NaH_2PO_4; 0.00116 g, $MgCl_2$ $6H_2O$; 0.02033 g, HEPES; 0.11 g and BSA; 0.35 g in 100 ml H_2O) and mixed well centrifuged for 20 min at 4500 g. The pellet was again suspended in tyrode albumin buffer pH 6.5 and centrifuged again for 20 min at 4500 g and the pellet obtained was suspended in tyrode albumin buffer pH 7.35 containing 2 mM $CaCl_2$ $6H_2O$ and this suspension was taken for platelet aggregation study.

2.2.7. Platelet aggregation

The turbidimetric method of Born [33] was followed using a Chronolog dual channel whole blood/optical LUMI aggregation system (Model-700). PRP aliquots were pre-incubated with various concentrations of DCT (0–3 µg) in the 0.25 ml reaction volume. The aggregation was initiated independently by the addition of agonists, such as collagen and ADP followed for 6 min. In another set, washed platelets aliquots were pre-incubated with various concentrations of DCT (0–3 µg) in the 0.25 ml reaction volume and the aggregation was initiated by the addition of thrombin followed for 6 min.

2.2.8. Molecular docking studies of benzothiazepinone series against thrombin target

We performed computational docking studies to investigate the molecular interactions between the benzothiazepinone series and thrombin. The whole set of 18 benzothiazepinones were prepared for docking using LigPrep 2.5 [34], keeping the default settings and using the Epik option that introduces energy penalties associated with ionization and tautomerization. The co-crystal structure of thrombin with 1-(2R)-2-amino-3-phenyl-propanoyl-N-(2,5-dichlorophenyl)methylpyrrolidine-2-carboxamide (PDB: 4UDW) was prepared for protein–ligand docking with Glide [35]. The structure was prepared using the Protein Preparation Wizard of Maestro 9.3 [36]. This was done following the default protocol taking into account energy refinement, hydrogen addition, pKa assignment, and side-chain rotational isomer refinement.

Table 1
Optimization of reaction conditions.[a]

Entry	Catalyst	Ligand	Time (h)	Yield[b] (%) C—N	Time (h)	Yield[c] (%) C—C
1	$Pd(OAc)_2$	L1	15	NR	15	NR
2	$Pd(Oac)_2$	L2	15	NR	15	19
3	$Pd(Oac)_2$	L3	15	21	15	NR
4	$Pd(Oac)_2$	L4	15	16	15	25
5	Pd_2dba_3	L1	15	NR	15	NR
6	Pd_2dba_3	L2	15	NR	15	43
7	Pd_2dba_3	L3	12	50	15	20
8	Pd_2dba_3	L4	12	80	15	34
9	Pd_2dba_3	L4	6	57	6	15
10	$Pd(PPh)_3Cl_2$	–	12	NR	15	31
11	$Pd(PPh)_3Cl_2$	L1	15	NR	15	NR
12	$Pd(PPh)_3Cl_2$	L2	15	NR	8	81
13	$Pd(PPh)_3Cl_2$	L3	15	NR	8	84
14	$Pd(PPh)_3Cl_2$	L4	15	NR	15	45

[a] Reaction condition: for C—N/C—C bond formation:- **2** (1 mmol), aniline/phenyl boronic acid/(1 mmol), ligand (0.1 equivalence), Pd Catalyst (0.05 equivalence) and Cs_2CO_3 2.5 equivalent, 1,4 Dioxane solvent at 100 °C for 8–15 h.

[b] Isolated yield for C—N coupled products.

[c] Isolated yield for C—C coupled products.

Table 2
Newly synthesized C−N coupled products.

Entry	Substrate 2	Amines (**3a-i**)	Products (**4a-i**)
1	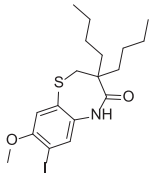	 **3a**	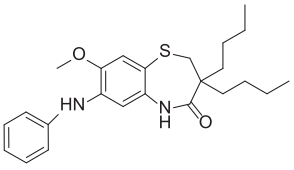 **4a**
2		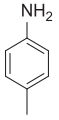 **3b**	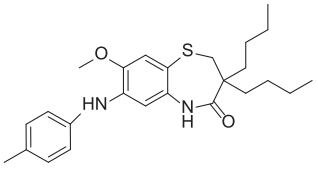 **4b**
3		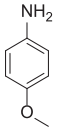 **3c**	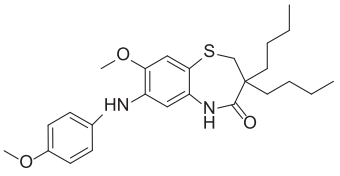 **4c**
4		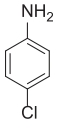 **3d**	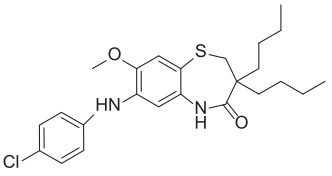 **4d**
5		 **3e**	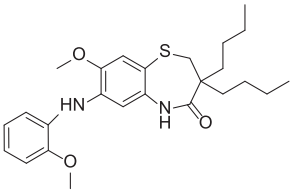 **4e**
6		 **3f**	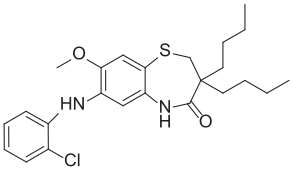 **4f**
7		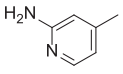 **3g**	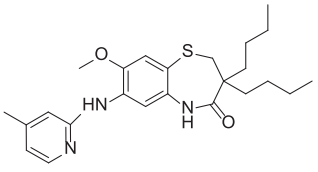 **4g**
8		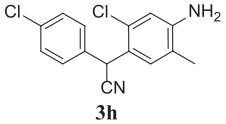 **3h**	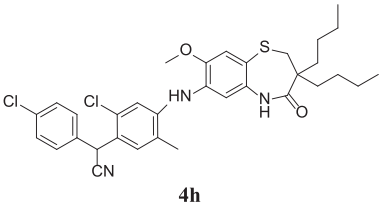 **4h**

(*continued on next page*)

Table 2 (*continued*)

Entry	Substrate 2	Amines (**3a-i**)	Products (**4a-i**)
9		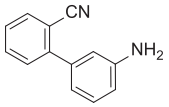 **3i**	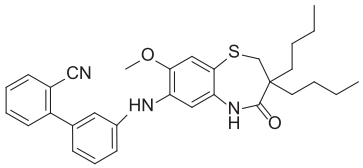 **4i**

Then resolved water molecules were discarded and the structure was centered using the co-crystallized ligand as the center of the receptor grid generated for the protein structure. The co-crystal structure of thrombin with 1-(2R)-2-amino-3-phenyl-propanoyl-N-(2,5-dichlorophenyl)methylpyrrolidine-2-carboxamide was selected as the target structure. The prepared Benzothiazepinones were docked into the active site of the thrombin with 1-(2R)-2-amino-3-phenyl-propanoyl-N-(2,5-dichlorophenyl)methylpyrrolidine-2-carboxamide (PDB: 4UDW) protein crystal structure. The Glide docking parameters were Glide score that included standard precision (SP) and the flexible ligand sampling option.

3. Results and discussion

3.1. Chemistry

3.1.1. Synthesis of 3,3-dibutyl-7-iodo-8-methoxy-2,3-dihydrobenzo [b] [1,4]thiazepin-4(5H)-one

Given the remarkable medicinal importance of benzothiazepines and continuation of efforts to explore the pharmacological properties of new heterocycles [37–43], in the present work, we synthesized a new series of benzothiazepine derivatives. Initially, we used a mild and selective method for the iodination [44] of 3,3-dibutyl-8-methoxy-2,3-dihydrobenzo[b] [1,4]thiazepin-4(5H)-one **(1)** using potassium-2-amino-5-methoxy benzenethiolate and 2-(bromomethyl) − 2-butylhexanoic acid to form 3,3-dibutyl-7-iodo-8-methoxy-2,3-dihydrobenzo[b] [1,4]thiazepin-4(5H)-one **(2)** with a yield of 71% (Fig. 2A).

The structure of **2** was determined by NMR and mass spectral analysis techniques and provided as supplementary information.

In the next step, we focussed on the derivatization of **(2)** via C−N and C−C bond formation reaction. Initially, we screened various classes of ligands (Fig. 2B) such as 1,10-Phenanthroline Diamine (L1), 2′-(Dicyclohexylphosphino)acetophenone ethylene ketal (L2, BINAP), 2,2′-bis(diphenylphosphino)-1,1′-binaphthyl (L3, Sympos) and 1,3-Bis (2,4,6-trimethylphenyl)imidazolinium Chloride (L4, *N*-heterocyclic carbine) for their ability to perform efficient coupling reactions. In these reactions, Cs_2CO_3 was kept as a common base for coupling reaction with a different palladium catalyst in 1,4-dioxane as a solvent. To verify this method, **(2)** and aniline were used as model substrates for C−N bond formation reaction, while **(2)** and phenylboronic acid for C−C coupling reaction (Table 1). We observed that substrates were transformed into the desired C−N coupled product in the presence of L3 and L4 (0.1 eq), and $Pd_2(dba)_3$ (0.05 eq) at 100 °C for 12 h. (Table 1, Entry 7 and 8.) Optimization of reaction conditions revealed that a combination of $Pd_2(dba)_3$ and L4 (Table1, Entry 8) efficiently transformed substrates to the corresponding C−N coupled product with a yield of 80%. The reduction in reaction time to 6h resulted in the subsequent decline in yield to 57% (Table 1, Entry 9).

We next optimized the reaction conditions for C−C bond formation. We found that use of $Pd(PPh)_3Cl_2$ as a catalyst converted substrate into the product in the absence of ligand (Table 1, Entry 10) with a yield of 31%. Further investigation on the choice of ligands revealed that the use of L2 and L3 in the particular base system for C−C cross-coupling reaction at 100 °C for 8 h resulted in efficient organic transformation with a yield of 81% and 84% (Table1, Entry 12 and 13). The reaction with other palladium catalysts and ligands resulted in a moderate yield of the product, despite longer reaction time and high temperature. Based on these results, we examined the generality of C−N bond forming reaction on **(2)** with different substituted aromatic amines (Table 2). It was observed that the products (**4a-f**), derived from electron-rich substituents of aromatic amines resulted in good yield (Fig. 3A). However, the use of heterocyclic amines **(3g)** and substituted biphenylamines **(3h and 3i)** resulted in only moderate conversion into products.

Further, the C−C bond formation reaction protocol was extended on

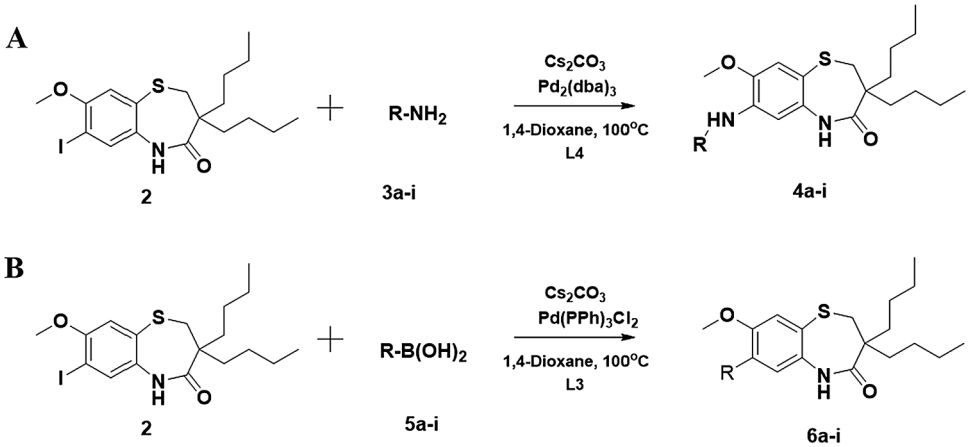

Fig. 3. Schematic representation of the synthesis and derivatization of dibutyl benzothiazepinone *via* (A) C−N bond formation reactions (B) C−C bond formation reactions.

Table 3
Newly synthesized C—C coupled products.

Entry	Substrate 2	Boronic acid (**5a-i**)	Products (**6a-i**)
1	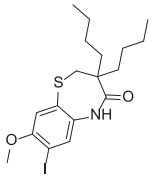	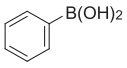 **5a**	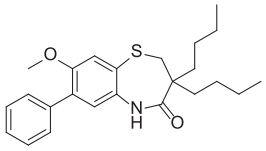
2		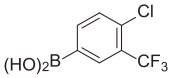 **5b**	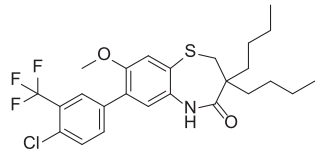
3		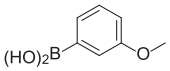 **5c**	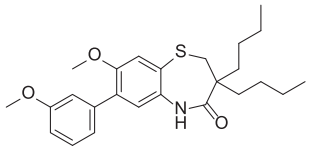
4		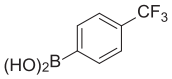 **5d**	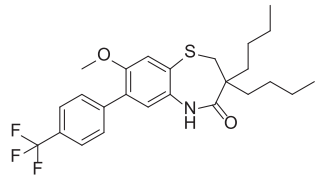
5		 **5e**	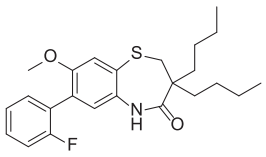
6		 **5f**	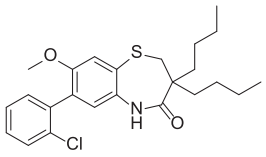
7		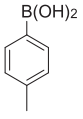 **5g**	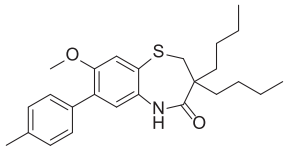
8		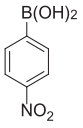 **5h**	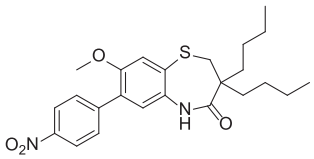 **6h**
9		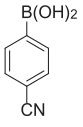 **5i**	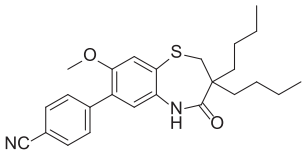 **6i**

(2) using various substituted aryl boronic acids (Table 3). Most of the reactions were completed within 8h with a good product yield (Fig. 3B). We observed the decrease in reaction efficiency for boronic acids bearing electron withdrawing groups **(5h and 5i)**, leading to poor conversion.

*3.1.2. X-ray crystal structure determination of **4g** and **6c***

Crystals of compound **4g** and **6c** were grown using slow evaporation technique. Using an X-ray diffractometer, the single crystal structures of **4g** (size: 0.3 × 0.27 × 0.25 mm) and **6c** (size: 0.29 × 0.27 × 0.25 mm) were solved by direct methods using SHELXS97 and successive least-

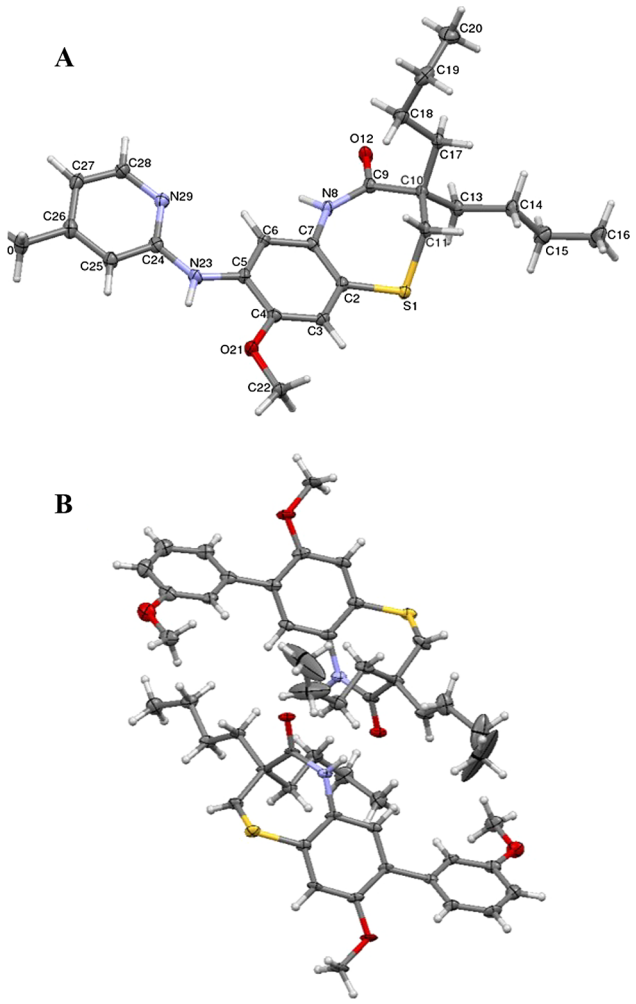

Fig. 4. ORTEP diagram of compound 4g (A) and 6c (B), based on single-crystal X-ray data.

squares full-matrix refinement was done using SHELXL97. The final refinement method for the full matrix least-squares on F^2 which explains the convergence implying the best fit including $R_1 = 0.0995$ and 0.0430, $R_2 = 0.2754$ and 0.1286 with goodness-of-fit 1.254 and 1.065 for the structures of 4g and 6c, respectively. The single crystal refinement data for the compounds **4g** and **6c** are provided as Supplementary Tables 1 and 2. The structures of compounds **4g** and **6c** are shown in Fig. 4A and B. The substituted phenyl rings at the 6 and 7 positions of 4g and 6c are planar.

3.2. Biological studies

3.2.1. In vitro screening against thrombin

Benzothiazepinone derivatives are known for their inhibitory activity towards platelet aggregation and underlying molecular mechanism still needs to be explored. Therefore, initially, all the newly synthesized benzothiazepinone derivatives were examined for their *in vitro* thrombin inhibitory activity at the concentration of 10 μM and the activity of thrombin was presented based on the fluorescence (RFU: Relative Fluorescence Unit) of the AMC-based peptide substrate. Among the newly synthesized library of benzothiazepinones, DCT (compound 6f) displayed the maximum thrombin inhibition with an IC_{50} value of 3.85 μM. Compounds 4e, 6d, 6e, and 6h displayed still significant but lesser inhibitory activity with an IC_{50} value of 4.86, 6.74, 8.02 and 15.75 respectively and marginal inhibition was observed by other derivatives (Fig. 5A). These results indicate that the biphenyl tethered benzothiazepinones having electron withdrawing groups showed potent inhibition towards thrombin except compound 6i (R = CN), whereas the reverse was the case for electron donating groups in the same position.

3.2.2. DCT prolongs the clotting time of human plasma

Thrombin is a serine protease that cleaves fibrinogen to form fibrin which is essential for blood coagulation. To firstly determine whether DCT possess anticoagulant activity, we performed a plasma recalcification assay, which detects the increase in clotting time of citrated human plasma in a concentration-dependent manner. We observed the maximum clotting time at 320 ± 11 sec in the sample treated with DCT (5 μg), compared to vehicle control with a clotting time of 200 ± 07 sec (Fig. 5B). These results indicate that DCT possesses anticoagulant activity.

3.2.3. Effect of DCT on activated partial thromboplastin time (APTT), and prothrombin time (PT)

Blood coagulation occurs through two pathways namely, extrinsic and intrinsic pathway. Since DCT exerts anticoagulant property, we further investigated the effect of DCT on both extrinsic and intrinsic coagulation pathways. In APTT assay, the addition of a negatively charged substance to plasma triggers activation of factor XII and sets off the intrinsic pathway of coagulation [45]. In PT assay, coagulation is triggered through the extrinsic pathway by adding tissue extracts to the plasma [45,46]. Both the coagulation pathways converge at the downstream event that leads to the activation of thrombin [31]. Therefore, we performed APTT and PT to evaluate the effect of DCT on intrinsic and extrinsic coagulation pathway. APTT is extended during the deficiency of any of the coagulation factors or in the presence of inhibitors of coagulation factors including prothrombin. To measure APTT, phospholipids preparation with ellagic acid and calcium ions was used for the activation of clotting factors and the effect of DCT (1–5 μg) was evaluated (see Table 4). The results demonstrated the delay in clot

Table 4
The effect of DCT on clotting time of normal human plasma.

DCT (μg)	PT (S)	PT (INR Values)	APTT (S)	APTT ratio	TCT (S)
0	11.5 ± 0.02	0.99 ± 0.02	37.3 ± 0.03	1.36 ± 0.03	25 ± 0.7
1	12.3 ± 0.03	1.06 ± 0.02	50.3 ± 0.03	1.83 ± 0.03	30 ± 0.4
2	12.9 ± 0.02	1.12 ± 0.01	58.0 ± 0.01	2.11 ± 0.01	37 ± 0.5
3	13.5 ± 0.01	1.17 ± 0.02	57.6 ± 0.02	2.09 ± 0.02	41 ± 1
4	14.5 ± 0.02	1.26 ± 0.01	55.6 ± 0.04	2.02 ± 0.04	49 ± 0.8
5	14.7 ± 0.01	1.28 ± 0.01	46.7 ± 0.03	1.70 ± 0.03	57 ± 1
Heparin (1 μg)	12.5 ± 0.2	–	49.6 ± 2.5	–	80.7 ± 4.9

PT: Prothrombin time; APTT: Activated partial thromboplastin time; INR: International normalized ratio; TCT: Thrombin clotting time. Heparin represents the positive control and the PT, APTT and TCT values for heparin is taken from a previous report [52].

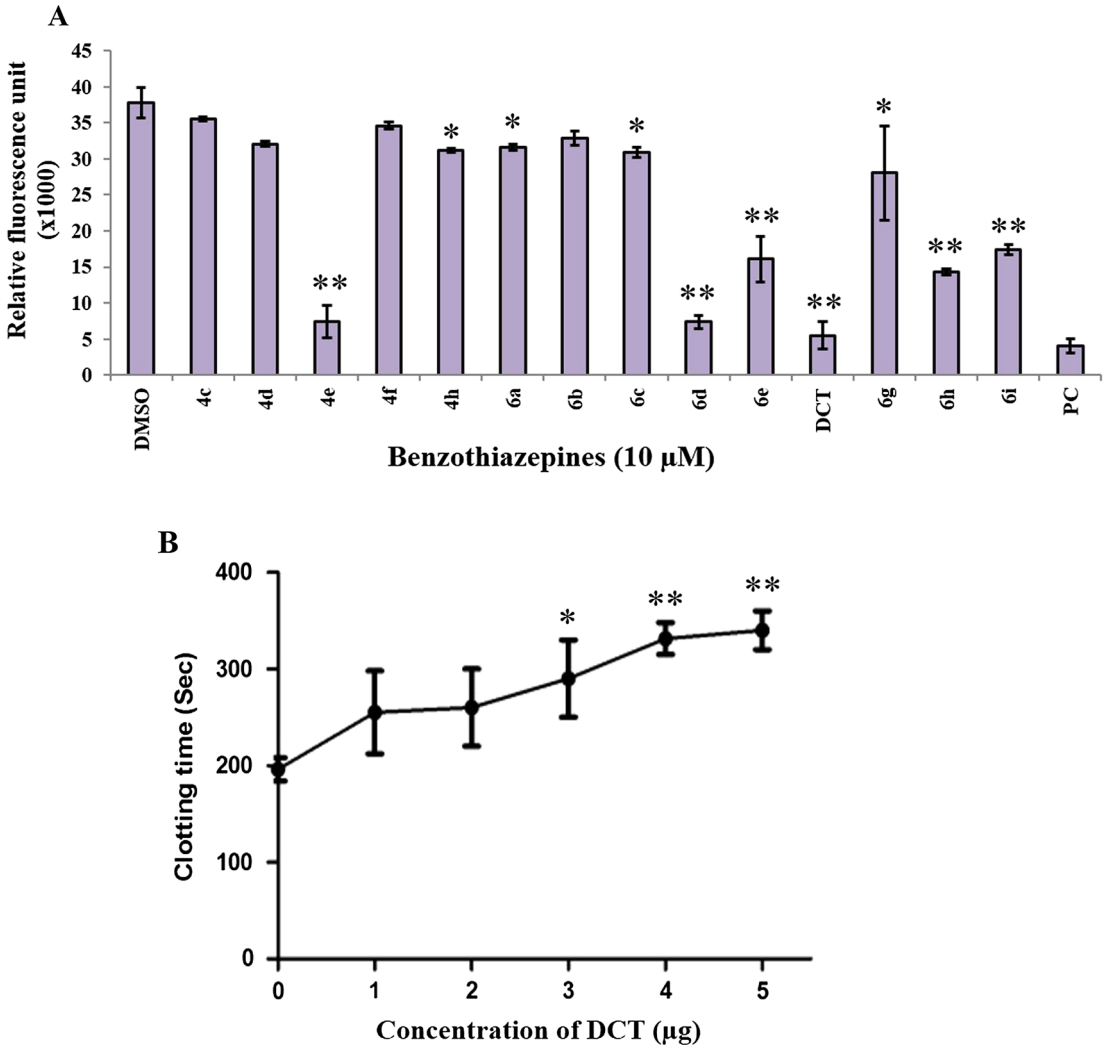

Fig. 5. (A) Screening of new benzothiazepinone derivatives against the activity of thrombin at 10 µl. The positive control is PPACK dihydrochloride. (B) DCT (0–5 µg) was pre-incubated with 0.2 ml of citrated human plasma in the presence of 20 µl 10 Mm Tris–HCl buffer pH 7.4 for 1 min at 37 °C. 20 µl of 0.25 M $CaCl_2$ was added to the pre-incubated mixture and clotting time was recorded. DCT prolongs the clotting time of human plasma. $^{*}P < 0.05$; $^{**}P < 0.01$.

formation on DCT (2 µg) treatment to 58 ± 0.01 s when compared with 37.3 ± 0.03 s in control. The PT was also found to be extended to 14.7 ± 0.01 s in DCT (5 µg) treated sample compared to 11.5 ± 0.02 s in the control. Overall, DCT prolonged the clot formation process in both APTT and PT with an increase in the concentration of DCT. These results suggest that DCT may inhibit thrombin in order to interfere with both the coagulation pathways.

3.2.4. Effect of DCT on thrombin clotting time (TCT)

TCT is a measure of the time taken for stable clot formation after the addition of thrombin to citrated plasma [47]. Thrombin converts fibrinogen to fibrin which is essential for the formation of a stable clot. TCT specifically allows the detection of thrombin or fibrin inhibitors [47]. Therefore, we next performed TCT to evaluate the effect of DCT on the formation of a stable clot. Interestingly, DCT prolonged the clot formation process of TCT from 25 ± 0.7 s (control) to 57 ± 1 s (DCT treated (5 µM), Table 4). The results clearly demonstrated that DCT significantly increases clotting time by interfering with the conversion of fibrinogen to fibrin. Therefore, it is evident that DCT induces anticoagulative activity *via* inhibition of thrombin.

3.2.5. Effect of DCT on agonist-induced platelet aggregation

To examine the effect of DCT on the function of platelets, we next evaluated the effect of DCT on agonist-induced platelet aggregation. Collagen, ADP, and thrombin were used as agonists of platelet aggregation in independent experiments. The pretreatment of PRP with various concentrations of DCT resulted in the inhibition of ADP- and collagen-induced platelet aggregation of about 62.0% and 98% respectively at the concentration of 3 µg/ml (Figs. 6 and 7). Similarly, the treatment of washed platelets with different concentrations of DCT resulted in the inhibition of thrombin-induced platelet aggregation of about 76% (Fig. 8). We also observed the inhibition of agonist-induced platelet aggregation in a dose-dependent manner (Table 2).

3.2.6. Molecular docking studies against thrombin

The benzothiazepinone series have consistently displayed hydrogen-bonding mode with Ser-214, which is similar to that of the co-crystallized ligand (PDB ID: 4UDW). Furthermore, additional trends in binding modes were observed for 6d and DCT (Fig. 9): Hydrogen bonding to Ser-195, and π-π interactions between the methoxyphenyl groups and Trp-60. In fact, DCT, which displayed the highest activity in the *in vitro* assay, has exhibited the highest docking score among the whole series

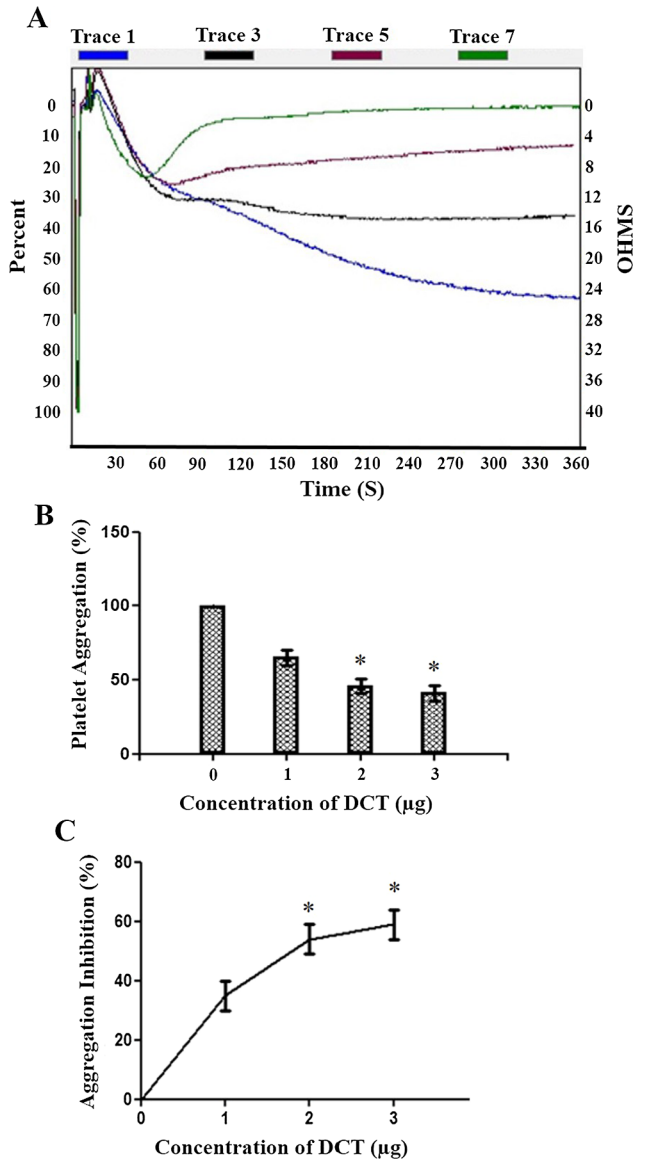

Fig. 6. DCT significantly downregulated ADP-induced platelet aggregation in a dosage-dependent manner. Platelet aggregation was initiated by adding ADP as an agonist to PRP. (A) Traces of platelet aggregation: Trace 1 (ADP 10 µM); Trace 3 (ADP 10 µM + 1 µg of DCT); Trace 5 (ADP 10 µM + 2 µg of DCT); Trace 7 (ADP 10 µM + 3 µg of DCT). The values represent ± SD of three independent experiments. (B) Dose-dependent platelet aggregation in percentage. (C) Dose-dependent platelet aggregation inhibition in percentage. $^{*}P < 0.05$.

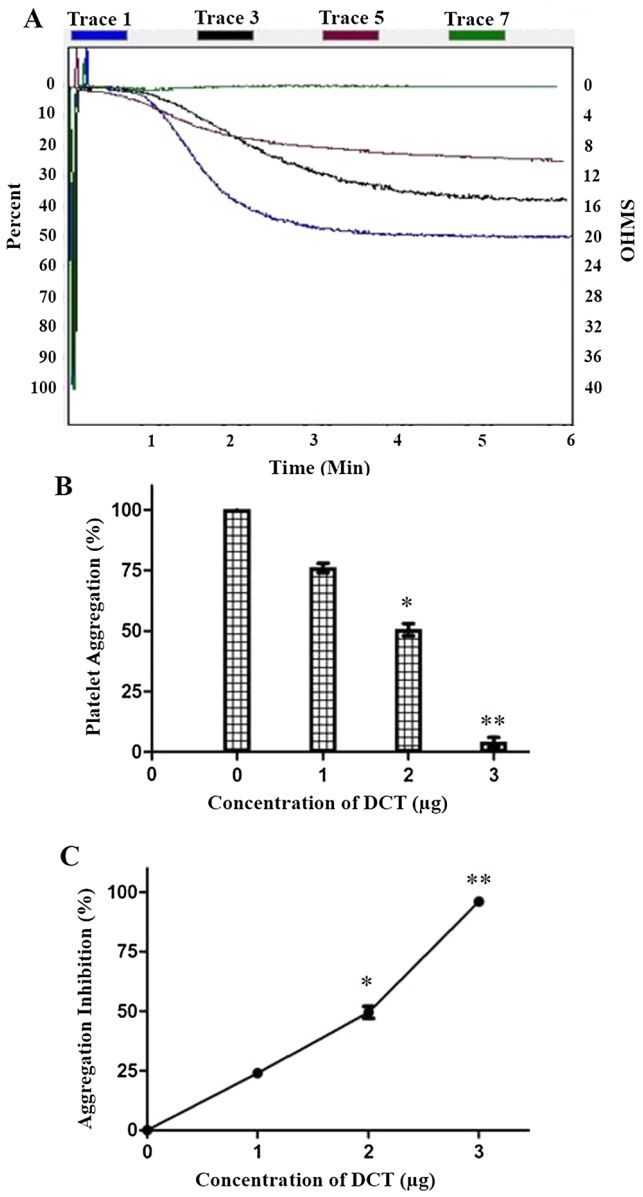

Fig. 7. DCT significantly downregulated collagen-induced platelet aggregation in a dosage-dependent manner. Platelet aggregation was initiated by adding collagen as an agonist to PRP. (A) Trace 1 (Collagen 2 µg/ml); Trace 3 (Collagen 2 µg/ml + 1 µg of DCT); Trace 5 (Collagen 2 µg/ml + 2 µg of DCT); Trace 7 (Collagen 2 µg/ml + 3 µg of DCT). The values represent ± SD of three independent experiments. (B) Dose-dependent platelet aggregation in percentage. (C) Dose-dependent platelet aggregation inhibition in percentage. $^{*}P < 0.05$; $^{**}P < 0.01$.

of compounds. It is noted that the hydrogen bonding interactions with the Ser-195 and Ser-214 exhibited by 6d and DCT are similar to those exhibited by another co-crystallized ligand of PDB ID: 1XMN. The distances from the carbonyl groups of 6d and DCT to the hydroxyl group of Ser-195 were computed, and they were 1.79 and 1.68 Å respectively, and from the amino groups of 6d and DCT to the carbonyl group of Ser-214, they were 1.89 and 1.98 Å respectively.

3.2.7. Statistical analysis

Using Origin 8 (OriginLab) software, the statistical analysis was carried out. The Mann–Whitney *U* test was used to determine P-values. $^{*}P < 0.05$ versus control. $^{**}P < 0.01$ versus control.

4. Conclusion

In the present study, we synthesized benzothiazepinone derivatives and evaluated their possible thrombin inhibitory activity. The results of the assay presented DCT as a potent thrombin inhibitor. The role of thrombin in coagulation is well-established and therefore we used various coagulation tests such as determination of plasma re-calcification time, prothrombin time, activated partial thromboplastin time and thrombin clotting time. Collagen, ADP, and thrombin are known inducers of platelet aggregation. Collagen induces platelet aggregation by interacting with its glycoprotein receptor on platelets and activates phospholipase C-mediated signaling cascade [48]. P2Y12 is a platelet

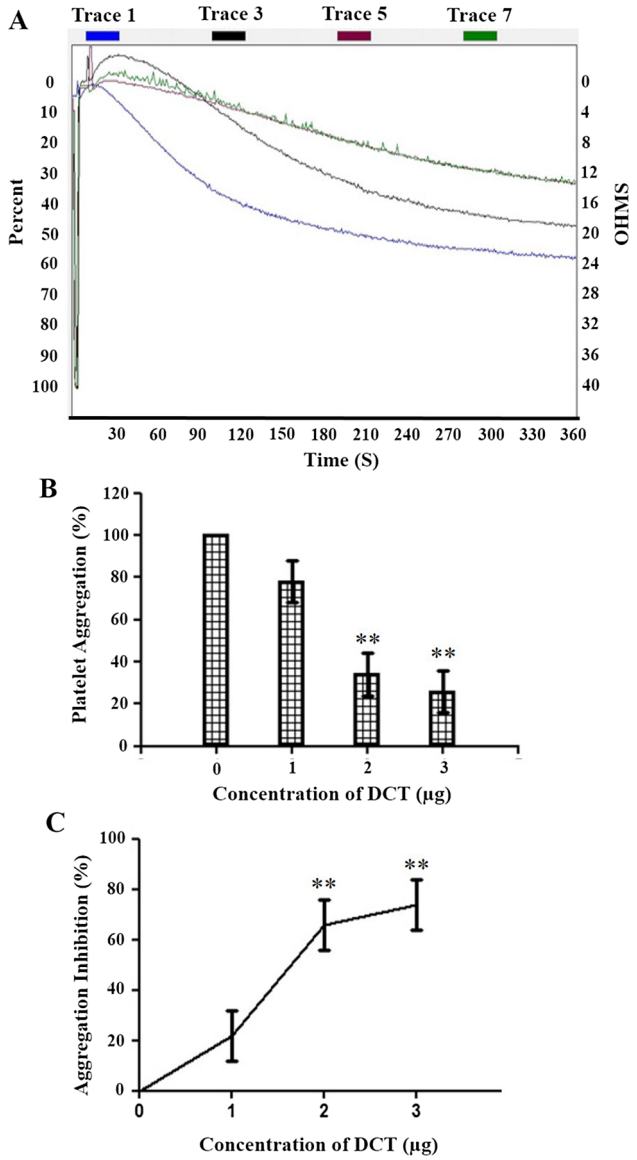

Fig. 8. DCT significantly downregulated thrombin-induced platelet aggregation in a dosage-dependent manner. Platelet aggregation was initiated by adding thrombin as an agonist to washed platelets. (A) Trace 1 (Thrombin 0.5 U/ml); Trace 3 (Thrombin 0.5 U + 1 µg of DCT); Trace 5 (Thrombin 0.5 U/ml + 2 µg of DCT); Trace 7 (Thrombin 0.5 U/ml + 3 µg of DCT). The values represent ± SD of three independent experiments. (B) Dose-dependent platelet aggregation in percentage. (C) Dose-dependent platelet aggregation inhibition in percentage. $^{**}P < 0.01$.

ADP receptor; Several antiplatelet small molecules such as thienopyridines (clopidogrel) inhibit P2RY12 signaling and suppress the ADP-induced platelet aggregation [49]. Thrombin inhibitors such as argatroban were reported to inhibit collagen-induced platelet activation and aggregation [50,51]. The treatment of DCT resulted in the inhibition of collagen, ADP, and thrombin-induced platelet aggregation. In summary, we report the synthesis of benzothiazepinone derivatives and evaluated all the new compounds for their thrombin inhibitory activity. The results presented DCT as a potent inhibitor of thrombin. The functional studies revealed that DCT possesses the antiplatelet effect. The molecular docking analysis revealed the putative interactions of DCT with thrombin. Since several thrombin inhibitors are associated with secondary complications in *in vivo* conditions, further comprehensive investigation is essential to understand the possible adverse effects of DCT and its off-targets.

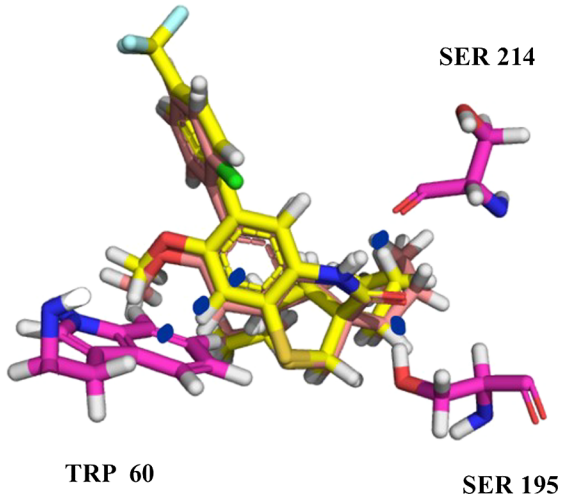

Fig. 9. 6d and DCT displayed the high activities against thrombin in the *in vitro* experiments, and the structural activity analysis revealed the predicted molecular interactions which are responsible for their activity: (A) Hydrogen bonding between the oxygen of the carbonyl and Ser-195 (B) Hydrogen bonding between the hydrogen of the amide and Ser-214 (C) π-π interactions between the methoxyphenyl groups and Trp-60.

Acknowledgments

This research was supported by Council of Scientific and Industrial Research (No. 02(0291)17/EMR-II), Department of Biotechnology (No. BT/PR/8064/BID/7/441/2013) and Vision group on Science and Technology, India to Basappa. This research was also supported by University Grants Commission-Israel Science Foundation to KSR and Shenzhen Development and Reform Commission Subject Construction Project [2017]1434 to PEL.

Conflict of interest

The authors declare no conflict of interest.

Author contributions

KSR, B, PEL, AB conceived the project. KSR, B, AB, SD, CDM designed the experiments. CPB, VP, SR, NS, LK carried out the research and analysis of data. KSR, B, AB, CDM, CPB, LK wrote the paper.

Appendix A. Supplementary material

Supplementary data to this article can be found online at https://doi.org/10.1016/j.bioorg.2019.03.004.

References

[1] N.H. Hauel, H. Nar, H. Priepke, U. Ries, J.-M. Stassen, W. Wienen, Structure-based design of novel potent nonpeptide thrombin inhibitors, J. Med. Chem. 45 (2002) 1757–1766.
[2] S. Palta, R. Saroa, A. Palta, Overview of the coagulation system, Indian J. Anaesth. 58 (2014) 515–523.
[3] B.F. Le Bonniec, Thrombin A2 – Rawlings, Neil D, in: G. Salvesen (Ed.), Handbook of Proteolytic Enzymes, Academic Press, 2013, pp. 2915–2932 (Chapter 643).
[4] E. Perzborn, S. Heitmeier, U. Buetehorn, V. Laux, Direct thrombin inhibitors, but not the direct factor Xa inhibitor rivaroxaban, increase tissue factor-induced hypercoagulability in vitro and in vivo, J. Thromb. Haemostasis: JTH 12 (2014) 1054–1065.
[5] G. Soslau, R. Class, D.A. Morgan, C. Foster, S.T. Lord, P. Marchese, Z.M. Ruggeri, Unique pathway of thrombin-induced platelet aggregation mediated by glycoprotein Ib, J. Biol. Chem. 276 (2001) 21173–21183.
[6] K.A. Tanaka, N.S. Key, J.H. Levy, Blood coagulation: hemostasis and thrombin regulation, Anesth. Analg. 108 (2009) 1433–1446.
[7] S. Alban, Adverse effects of heparin, in: R. Lever, B. Mulloy, C.P. Page (Eds.), Heparin – A Century of Progress, Springer, Berlin, Heidelberg, 2012, pp. 211–263.

[8] D.K. Wysowski, P. Nourjah, L. Swartz, Bleeding complications with warfarin use: a prevalent adverse effect resulting in regulatory action, Arch. Intern. Med. 167 (2007) 1414–1419.
[9] M. Di Nisio, S. Middeldorp, H.R. Buller, Direct thrombin inhibitors, New Engl. J. Med. 353 (2005) 1028–1040.
[10] G. Helft, T. Lecompte, C. Le Feuvre, J.P. Metzger, A. Vacheron, M.M. Samama, Anti-streptokinase antibodies, Arch. des maladies du coeur et des vaisseaux 90 (1997) 975–980.
[11] M.S. Dykewicz, K.G. McGrath, R. Davison, K.J. Kaplan, R. Patterson, Identification of patients at risk for anaphylaxis due to streptokinase, Arch. Intern. Med. 146 (1986) 305–307.
[12] K. Uchino, A.V. Hernandez, Dabigatran association with higher risk of acute coronary events: meta-analysis of noninferiority randomized controlled trials, Arch. Intern. Med. 172 (2012) 397–402.
[13] S. Schulman, K. Wahlander, T. Lundstrom, S.B. Clason, H. Eriksson, Secondary prevention of venous thromboembolism with the oral direct thrombin inhibitor ximelagatran, New Engl. J. Med. 349 (2003) 1713–1721.
[14] V. Gurewich, Ximelagatran—promises and concerns, JAMA 293 (2005) 736–739.
[15] T. Petzold, M. Thienel, I. Konrad, I. Schubert, R. Regenauer, B. Hoppe, M. Lorenz, A. Eckart, S. Chandraratne, C. Lennerz, C. Kolb, D. Braun, J. Jamasbi, R. Brandl, S. Braun, W. Siess, C. Schulz, S. Massberg, Oral thrombin inhibitor aggravates platelet adhesion and aggregation during arterial thrombosis, Sci. Transl. Med. 8 (2016) 367ra168.
[16] P. Zhang, H.-R. Hu, S.-H. Bian, Z.-H. Huang, Y. Chu, D.-Y. Ye, Design, synthesis and biological evaluation of benzothiazepinones (BTZs) as novel non-ATP competitive inhibitors of glycogen synthase kinase-3β (GSK-3β), Eur. J. Med. Chem. 61 (2013) 95–103.
[17] D. Saha, G. Jain, A. Sharma, Benzothiazepines: chemistry of a privileged scaffold, RSC Adv. 5 (2015) 70619–70639.
[18] T. Li, J. Zhang, J. Pan, Z. Wu, D. Hu, B. Song, Design, synthesis, and antiviral activities of 1,5-benzothiazepine derivatives containing pyridine moiety, Eur. J. Med. Chem. 125 (2017) 657–662.
[19] M. Bakthadoss, G. Murugan, Simple and new protocol for the synthesis of novel (z)-3-arylidenebenzothiazepin-4-ones using Baylis-Hillman derivatives, Synth. Commun. 38 (2008) 3406–3413.
[20] A.R. Katritzky, H.H. Odens, S. Zhang, C.J. Rostek, O.W. Maender, Novel syntheses of 2,3-Dihydro-1,5-benzothiazepin-4(5H)-ones and 2H–1,4-Benzothiazin-3(4H)-ones, J. Organ. Chem. 66 (2001) 6792–6796.
[21] K.H.M. Sampath, C.P. Pawan, R.M. Shesha, J. Sipak, J.S. Yadav, Solid Phase synthesis of hydroxy benzothiazepinones through cyclative release under thermolysis, Chem. Lett. 33 (2004) 888–889.
[22] S.-J. Tu, X.-D. Cao, W.-J. Hao, X.-H. Zhang, S. Yan, S.-S. Wu, Z.-G. Han, F. Shi, An efficient and chemoselective synthesis of benzo[e] [1,4] thiazepin-2(1H,3H,5H)-ones via a microwave-assisted multi-component reaction in water, Org. Biomol. Chem. 7 (2009) 557–563.
[23] M. Katoh, T. Karasawa, H. Doi, A. Odawara, M. Takagi, T. Ikeo, H. Narita, Antiplatelet mechanisms of TA-993 and its metabolite MB3 in ADP-induced platelet aggregation, Eur. J. Pharmacol. 399 (2000) 91–96.
[24] G. Anfossi, M. Trovati, E. Mularoni, P. Massucco, F. Cavalot, L. Mattiello, G. Emanuelli, Studies on inhibition of human platelet response by diltiazem, Gen. Pharmacol. 21 (1990) 949–954.
[25] H. Ono, M. Kimura, Effect of Ca2+-antagonistic vasodilators, diltiazem, nifedipine, perhexiline and verapamil, on platelet aggregation in vitro, Arzneimittelforschung 31 (1981) 1131–1134.
[26] R. Kaur, R. Singh, K. Singh, 1, 5-Benzothiazepine: bioactivity and targets, Chem. Biol. Lett. 3 (2016) 18–31.
[27] A. Odawara, K. Kikkawa, M. Katoh, H. Toryu, T. Shimazaki, Y. Sasaki, Inhibitory effects of TA-993, a new 1,5-benzothiazepine derivative, on platelet aggregation, Circ. Res. 78 (1996) 643.
[28] J.B. Bariwal, K.D. Upadhyay, A.T. Manvar, J.C. Trivedi, J.S. Singh, K.S. Jain, A.K. Shah, 1,5-Benzothiazepine, a versatile pharmacophore: a review, Eur. J. Med. Chem. 43 (2008) 2279–2290.
[29] J.S. Schroeder, W.H. Frishman, J.D. Parker, D.J. Angiolillo, C. Woods, B.M. Scirica, Pharmacologic options for treatment of ischemic disease A2 - Antman, Elliott M, in: M.S. Sabatine (Ed.), Cardiovascular Therapeutics: A Companion to Braunwald's Heart Disease, fourth ed. W.B. Saunders, Philadelphia, 2013, pp. 83–130 (Chapter 7).
[30] R.G. McKeever, R.J. Hamilton, Calcium channel blockers, StatPearls, StatPearls Publishing StatPearls Publishing LLC., Treasure Island (FL), 2018.
[31] S. Devaraja, K.S. Girish, M.S. Santhosh, M. Hemshekhar, S.C. Nayaka, K. Kemparaju, Fusaric acid, a mycotoxin, and its influence on blood coagulation and platelet function, Blood Coagul. Fibrin. Int. J. Haemostasis Thromb. 24 (2013) 419–423.
[32] N. Ardlie, P. Han, Enzymatic basis for platelet aggregation and release: the significance of the 'platelet atmosphere' and the relationship between platelet function and blood coagulation, Br. J. Haematol. 26 (1974) 331–356.
[33] G.V.R. Born, Aggregation of blood platelets by adenosine diphosphate and its reversal, Nature 194 (1962) 927–929.
[34] S. Schrödinger Release 2016-4, LigPrep, LLC, New York, NY, 2016.
[35] T.A. Halgren, R.B. Murphy, R.A. Friesner, H.S. Beard, L.L. Frye, W.T. Pollard, J.L. Banks, Glide: a new approach for rapid, accurate docking and scoring. 2. Enrichment factors in database screening, J. Med. Chem. 47 (2004) 1750–1759.
[36] G.M. Sastry, M. Adzhigirey, T. Day, R. Annabhimoju, W. Sherman, Protein and ligand preparation: parameters, protocols, and influence on virtual screening enrichments, J. Comput. Aided Mol. Des. 27 (2013) 221–234.
[37] K.S. Rakesh, S. Jagadish, T.R. Swaroop, C.D. Mohan, N. Ashwini, K.B. Harsha, F. Zameer, K.S. Girish, K.S. Rangappa, Anti-cancer activity of 2,4-disubstituted thiophene derivatives: dual inhibitors of lipoxygenase and cyclooxygenase, Med. Chem. (Shariqah (United Arab Emirates)) 11 (2015) 462–472.
[38] S. Anusha, C.D. Mohan, H. Ananda, C.P. Baburajeev, S. Rangappa, J. Mathai, J.E. Fuchs, F. Li, M.K. Shanmugam, A. Bender, G. Sethi, Basappa, K.S. Rangappa, Adamantyl-tethered-biphenylic compounds induce apoptosis in cancer cells by targeting Bcl homologs, Bioorg. Med. Chem. Lett 26 (2016) 1056–1060.
[39] N.C. Anilkumar, M.S. Sundaram, C.D. Mohan, S. Rangappa, K.C. Bulusu, J.E. Fuchs, K.S. Girish, A. Bender, Basappa, K.S. Rangappa, A one Pot synthesis of novel bioactive tri-substitute-condensed-imidazopyridines that targets snake venom phospholipase A2, PloS one 10 (2015) e0131896.
[40] K.S. Rakesh, S. Jagadish, K.S. Balaji, F. Zameer, T.R. Swaroop, C.D. Mohan, S. Jayarama, K.S. Rangappa, 3,5-disubstituted isoxazole derivatives: potential inhibitors of inflammation and cancer, Inflammation 39 (2016) 269–280.
[41] A. Sebastian, V. Pandey, C.D. Mohan, Y.T. Chia, S. Rangappa, J. Mathai, C.P. Baburajeev, S. Paricharak, L.H. Mervin, K.C. Bulusu, J.E. Fuchs, A. Bender, S. Yamada, Basappa, P.E. Lobie, K.S. Rangappa, Novel adamantanyl-based thiadiazolyl pyrazoles targeting EGFR in triple-negative breast cancer, ACS Omega 1 (2016) 1412–1424.
[42] S. Anusha, B. Cp, C.D. Mohan, J. Mathai, S. Rangappa, S. Mohan, S. Chandra, L. Paricharak, J.E. Mervin, M.M. Fuchs, A. Bender, Basappa, K.S. Rangappa, A nano-MgO and ionic liquid-catalyzed 'green' synthesis protocol for the development of adamantyl-imidazolo-thiadiazoles as anti-tuberculosis agents targeting sterol 14alpha-demethylase (CYP51), PloS one 10 (2015) e0139798.
[43] K.N. Nandeesh, H.A. Swarup, N.C. Sandhya, C.D. Mohan, C.S. Pavan Kumar, M.N. Kumara, K. Mantelingu, S. Ananda, K.S. Rangappa, Synthesis and anti-proliferative efficiency of novel bis(imidazol-1-yl)vinyl-1,2,4-oxadiazoles, New J. Chem. 40 (2016) 2823–2828.
[44] R. Badri, M. Gorjizadeh, A mild, efficient and selective iodination of aromatic compounds using iodine and 1,4-bis(triphenylphosphonium)-2-butene peroxodisulfate, Chin. Chem. Lett. 20 (2009) 1439–1443.
[45] A.P. Wheeler, D. Gailani, The intrinsic pathway of coagulation as a target for antithrombotic therapy, Hematol. Oncol. Clin. North Am. 30 (2016) 1099–1114.
[46] A.S. Wolberg, A.E. Mast, Tissue factor and factor VIIa–hemostasis and beyond, Thromb. Res. 129 (Suppl 2) (2012) S1–S4.
[47] V. Ignjatovic, Thrombin clotting time, Methods in molecular biology 992 (2013) 131–138.
[48] K. Sangkuhl, A.R. Shuldiner, T.E. Klein, R.B. Altman, Platelet aggregation pathway, Pharmacogenet. Genomics 21 (2011) 516–521.
[49] J.M. Herbert, P. Savi, P2Y12, a new platelet ADP receptor, target of clopidogrel, Semin. Vasc. Med. 3 (2003) 113–122.
[50] K. Umemura, H. Kawai, H. Ishihara, M. Nakashima, Inhibitory effect of clopidogrel, vapiprost and argatroban on the middle cerebral artery thrombosis in the rat, Jpn. J. Pharmacol. 67 (1995) 253–258.
[51] M. Imiya, T. Matsuo, Inhibition of collagen-induced platelet aggregation by argatroban in patients with acute cerebral infarction, Thromb. Res. 88 (1997) 245–250.
[52] Z.M. Wang, L. Li, B.S. Zheng, N. Normakhamatov, S.Y. Guo, Preparation and anticoagulation activity of sodium cellulose sulfate, Int. J. Biol. Macromol. 41 (2007) 376–382.